Ocean Engineering 159 (2018) 129–138

Contents lists available at ScienceDirect

Ocean Engineering

journal homepage: www.elsevier.com/locate/oceaneng

Numerical investigation of ventilated cavitating vortex shedding over a bluff body

Zhiying Wang [a], Biao Huang [a,*], Mindi Zhang [a], Guoyu Wang [a], Bin Ji [b]

[a] School of Mechanical and Vechicular Engineering, Beijing Institute of Technology, 5 South Zhongguancun Street, Beijing, 100081, China
[b] State Key Lab of Water Resources and Hydropower Engineering Science, Wuhan University, Wuhan, 430072, China

ARTICLE INFO

Keywords:
Ventilated cavitating flow
Vortex shedding
Lagrangian coherent structures

ABSTRACT

The objective of this paper is to investigate ventilated cavitating vortex shedding dynamics over a bluff body at $Re = 6.7 \times 10^4$ with large eddy simulation (LES) model. The finite-time Lyapunov exponent (FTLE) and Lagrangian coherent structures (LCS) methods are applied to investigate the formation, evolution and shedding of ventilated cavitating vortices. The results show that ventilated cavitation plays an important role in the vortex structures and the vortex shedding process. Comparing with non-cavitating flow, the Strouhal number *St* corresponding to vortex shedding increases and the length of formation region decreases when the gas entrainment coefficient is $Q_v = 0.0231$. While with further increase of gas entrainment coefficient, the *St* reduces gradually and the formation region expands. Based on the Lagrangian analysis of vortex dynamics, it can clearly be seen that the turbulent wake can be divided into two parts: near wake (the formation and development of vortices) and far wake (vortex street). The variation of the size of near wake is the same as that of the formation region. In the far wake, the vortices stretch and distort, and the rotation of vortices in the ventilated cavitating flow is not evident as that in non-cavitating flow.

1. Introduction

Ventilated cavitation is obtained by injecting gas into the low pressure regions of liquid flows (Franc and Michel, 2005). It is an interest topic due to its importance in a wide range of fundamental studies and engineering applications (Ceccio, 2009; Arndt et al., 2009; Mäkiharju et al., 2013; Karn et al., 2016b; Shao and Arndt et al., 2017; Barbaca et al., 2017; Liu et al., 2017; Wang et al., 2015). Wosnik and Arndt (2013) carried out experiments in high-speed water tunnel to investigate the interaction between a ventilated supercavity and its turbulent bubbly wake. Karn et al. (2016a) investigated the physical mechanisms of closure formation and transition in ventilated supercavity. When gas entrainment coefficient is not large enough to form a supercavity, cavitation often results in the formation of vortex shedding showing an unsteady behavior. Harwood et al. (2016) investigated the topology, formation, elimination and stability of ventilated cavity on a surface-piercing hydrofoil. The results indicated that the re-entrant jet played an important role in the stability of ventilated regimes. Although cavitation shedding dynamics has been extensively studied both experimentally and numerically (Arndt et al., 2000; Gopalan and Katz, 2000; Laberteaux and Ceccio, 2001; Lyer and Ceccio, 2002; Ji et al., 2013; Huang et al., 2013; Chen et al., 2016; Wang et al., 2017a,b,c; Wu et al., 2018), relatively fewer studies exist for the ventilated cavitation behind a bluff body. As the flow passes over a bluff body, various kinds of vortices form, develop and interact with each other in the wake, which will lead to vibration, noise, large fluctuating pressure forces, or resonance (Williamson, 1966; Balachandar and Ramamuthy, 1999; Brandner et al., 2010; Ganesh et al., 2016; Huang et al., 2014).

The characteristics of vortex shedding in non-cavitating flows over a bluff body have been widely studied (Gerrard, 1966; Yarusevych et al., 2009). It is well known that the fluid dynamics past a bluff body are complex, which involve the interaction of the boundary layer, the free-shear layer, and the wake. However, cavitating flow is one kind of multiphase flow, and so the fluid dynamics in the bluff-body wake are physically more complicated. Belahadji et al. (1995) investigated global conditions of inception and development of cavitation in the rotational structures of the turbulent wake. They found that the Strouhal number and vortex street depended strongly on the development of cavitation. Cavitation tended to change the flow features in the turbulent wake and made the local mechanism more complex in some extent. Ausoni et al. (2007) concentrated mainly on the effects of cavitation development and fluid-structure interaction on the

* Corresponding author.
E-mail address: huangbiao@bit.edu.cn (B. Huang).

https://doi.org/10.1016/j.oceaneng.2018.03.087
Received 8 October 2017; Received in revised form 28 March 2018; Accepted 31 March 2018

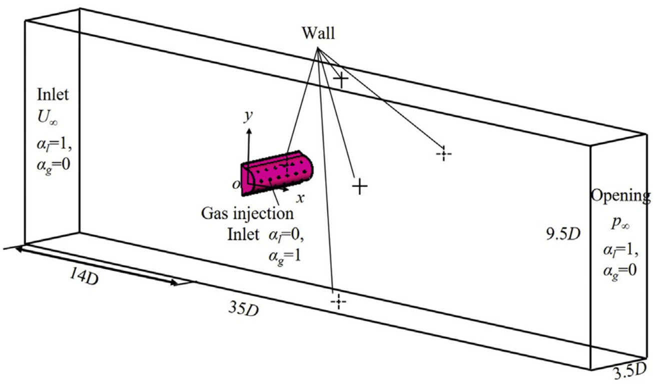

Fig. 1. Computational domain and boundary condition.

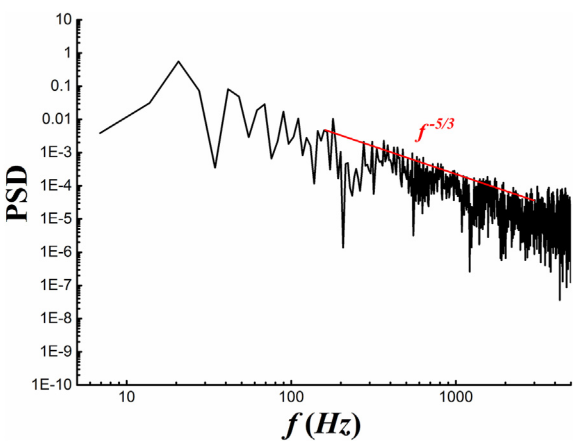

Fig. 2. The PSD analysis of the pressure fluctuation at the point $x/D = 0.6$.

mechanism of the vortex generation. They found that for fully developed cavitation, the vortex shedding frequency increased up to 15%, which was accompanied by the increase of the vortex advection velocity and reduction of the streamwise vortex spacing. Gnanaskandan and Mahesh (2016) demonstrated that cavitation effected the evolution of pressure, boundary layer and loads on the cylinder surface. In addition, cavitation suppressed turbulence and delayed the 3D breakdown of Kármán vortices. The literature above all indicated that cavitation had a significant influence on the fluid dynamics in the turbulent wake behind a bluff body. However, except for several studies, there has been relatively less research on the phenomenon of cavitating vortex shedding behind a bluff body, especially ventilated cavitating vortex shedding. The characteristics of ventilated cavitating vortex shedding over a bluff body are still not well understood.

As there are strong correlations between ventilated cavitation and vortex structures, it is important to identify regions of separated flow as well as wake structures to reveal the unsteady vortex behaviors in cavitating flow (Huang and Green, 2015; Cheng et al., 2018; Long et al., 2018). During these years, the finite-time Lyapunov exponent (FTLE) and Lagrangian Coherent Structures (LCS) methods are developed to study the intrinsic structures or properties within flows (Haller, 2001; Shadden et al., 2005). Green et al. (2007) demonstrated that the LCS method could define time-dependent vortex structure boundaries without relying on a pre-selected threshold, and presented greater visible details without the requirement of velocity derivatives. Brunton and Rowley (2009) applied LCS to visualize the relevant flow in the wake of a flat plate. Recently, some researchers gradually applied the FTLE and Lagrangian Coherent Structures (LCS) methods in cavitating flow. Tang et al. (2012) utilized the LCS method to flow dynamics and underlying physics of unsteady turbulent cavitating flows. These researches showed that the LCS was a powerful method to help identify and add the description of the dynamical features of different vortex-dominated flow fields.

In this work, the main goal is to improve the understanding of characteristics of ventilated cavitating vortex shedding over a bluff body. The paper is organized as follows. Section 2 is the numerical method. Sections 3 shows the numerical setups and descriptions. In Section 4, the FTLE is applied to display the influence of ventilated cavitation on the formation, evolution and shedding of vortices. In addition, the relationship between the vortex shedding process and unsteady loads is discussed.

2. Numerical model

The numerical results shown in this paper are performed using the commercial CFD code, CFX. to solve the unsteady Navier–Stokes equations by the LES Wall-Adapting Local Eddy-Viscosity (WALE) model (Nicoud and Ducros, 1999). The homogeneous model assumes that the transported quantities (with the exception of volume fraction) for that process are the same for all. The governing equations are shown as follows:

$$\frac{\partial \rho_m}{\partial t} + \frac{\partial(\rho_m u_j)}{\partial x_j} = 0 \tag{1}$$

$$\frac{\partial(\rho_m u_i)}{\partial t} + \frac{\partial(\rho_m u_i u_j)}{\partial x_j} = -\frac{\partial p}{\partial x_i} + \frac{\partial}{\partial x_j}\left(\mu_m \frac{\partial u_i}{\partial x_j}\right) \tag{2}$$

Here u is the velocity, p is the pressure, the mixtured density ρ_m and dynamic viscosity μ_m are defined as:

$$\rho_m = \rho_l \alpha_l + \rho_g \alpha_g \tag{3}$$

$$\mu_m = \mu_l \alpha_l + \mu_g \alpha_g \tag{4}$$

where, ρ_l is the liquid density, ρ_g is the gas density, which is a function of pressure and temperature. α_l is the liquid fraction, α_g is the gas fraction. $\alpha_l = 1 - \alpha_g$.

Applying a Favre-filtering operation to Equs.(1) and (2) gives the LES equations,

$$\frac{\partial \rho}{\partial t} + \frac{\partial(\rho \overline{u}_j)}{\partial x_j} = 0 \tag{5}$$

$$\frac{\partial(\rho \overline{u}_i)}{\partial t} + \frac{\partial(\rho \overline{u}_i \overline{u}_j)}{\partial x_j} = -\frac{\partial p}{\partial x_i} + \frac{\partial}{\partial x_j}\left(\mu \frac{\partial \overline{u}_i}{\partial x_j}\right) - \frac{\partial \tau_{ij}}{\partial x_j} \tag{6}$$

where, over-bar denotes a filtered quantity. By comparing Equ. (2) with Equ. (6), there is an extra nonlinear term τ_{ij}, which is called the sub-grid scale (SGS) stress. It includes the effect of the small scales and is defined by:

$$\tau_{ij} = \rho \overline{u_i u_j} - \overline{u_i}\,\overline{u_j} \tag{7}$$

The large scale turbulent flow is solved directly and the influence of the small scales is taken into account by appropriate subgrid-scale (SGS) models. An eddy viscosity approach is used which relates the subgrid-scale stresses τ_{ij} to the large-scale strain rate tensor $\overline{S}_{ij}$ in the following way:

$$\tau_{ij} - \frac{1}{3}\tau_{kk}\delta_{ij} = -2\mu_t \overline{S}_{ij} \tag{8}$$

$$\overline{S}_{ij} = \frac{1}{2}\left(\frac{\partial \overline{u}_i}{\partial x_j} + \frac{\partial \overline{u}_j}{\partial x_i}\right) \tag{9}$$

The $\overline{S}_{ij}$ is the rate-of-strain tensor for the resolved scale and the sub-